Surface electrical conduction due to carrier doping into a surface-state band on Si(111)-$\sqrt{3}\times\sqrt{3}$-Ag

Yuji Nakajima,* Sakura Takeda, Tadaaki Nagao, and Shuji Hasegawa†
Department of Physics, School of Science, University of Tokyo, 7-3-1 Hongo, Bunkyo-ku, Tokyo 113, Japan

Xiao Tong‡
Core Research for Evolutional Science and Technology, The Japan Science and Technology Corporation, Kawaguchi Center Building, Hon-cho 4-1-8, Kawaguchi, Saitama 332, Japan

(Received 14 April 1997; revised manuscript received 16 May 1997)

Photoemission spectroscopy has shown that each Ag atom in its two-dimensional adatom gas (2DAG) phase deposited on the Si(111)-$\sqrt{3}\times\sqrt{3}$-Ag surface at room temperature donates one electron into an antibonding surface-state band of this substrate, resulting in a steep increase in electrical conductance through the band. The surface space-charge layer makes no contribution to the conductance increase by the 2DAG adsorption, estimated from the band-bending measurements. When the 2DAG nucleates into three-dimensional Ag microcrystals by further deposition beyond a critical supersaturation coverage, the carrier-doping effect vanishes, returning to a lower conductance. These results reveal that the surface state acts as a *surface conduction band*. The electron mobility in this band is estimated to be on the order of 10 cm^2/V s. [S0163-1829(97)07935-6]

I. INTRODUCTION

In a previous paper[1] it was shown that Ag adatoms, deposited onto the Si(111)-$\sqrt{3}\times\sqrt{3}$-Ag surface at room temperature (RT), continued to exist as a supersaturated metastable two-dimensional gas phase when its coverage was below a critical coverage Θ_c (approximately 0.03 ML). This two-dimensional adatom gas (2DAG) was found to increase remarkably the surface electrical conductance. When the coverage exceeded Θ_c, the 2DAG nucleated into three-dimensional (3D) Ag microcrystals, returning the surface to an almost bare $\sqrt{3}\times\sqrt{3}$-Ag surface. The electrical conductance then returned to a lower value near the initial one, corresponding to a very low density of the Ag adatom gas equilibrated with the 3D microcrystals. It was thus concluded that only the isolated Ag adatoms before nucleation made the electrical conductance very high.

However, its mechanism is not yet clarified. The coverage ($\leqslant$ 0.03 ML) of the 2DAG is too small to make 2D percolation paths on a triangular lattice.[2] So the observed increase in conductance should be attributed to the substrate; the surface space-charge layer and/or the surface-state band should play a decisive role in the conductance changes. If the Ag adatoms in its 2DAG phase donate the excess carriers into the surface space-charge layer by inducing strong band bending, the observed increase in conductance would be naturally understood. An alternative scenario for the increase is that the Ag adatoms donate the carriers into a surface-state band, not into the bulk bands (surface space-charge layer). The electrical conduction via a surface-state band inherent to the $\sqrt{3}\times\sqrt{3}$-Ag substrate can be enhanced by adatom adsorption. This paper clarifies that the latter scenario, the enhancement of surface-state conductance due to electron doping by adsorbates, works for the present system. A surface-state band originating from an antibonding state between Ag and Si atoms in the $\sqrt{3}\times\sqrt{3}$-Ag structure works as a *surface conduction band*. This conclusion has been derived by measurements combined with x-ray photoelectron spectroscopy (XPS) to evaluate the band bending and angle-resolved ultraviolet photoelectron spectroscopy (ARUPS) to analyze the surface electronic structure near the Fermi level (E_F).

II. EXPERIMENT

An n-type Si(111) wafer with nominal resistivity of 11–100 Ω cm and $25\times3.7\times0.5$ mm^3 in size was used. The surface was cleaned to obtain a clear 7×7 reflection high-energy electron diffraction (RHEED) pattern, by several flash heatings up to 1500 K for 10 s with a direct current of about 8 A through it. The $\sqrt{3}\times\sqrt{3}$-Ag surface was prepared by 1-ML-Ag deposition with a constant rate of 0.2 ML/min onto the 7×7 substrate at 770 K. Substrate temperatures higher than 700 K were measured with an optical pyrometer, with an estimated accuracy of ±10 K. After switching off the heating current for the surface preparations, we waited for about 1.5 h to attain an isothermal condition at RT, which was confirmed by measuring the resistance changes of the Si wafer during the cooling process. The deposited amount of Ag was estimated by deposition duration with a constant deposition rate under an assumption of 1 ML of Ag needed for a complete conversion from the 7×7 structure to the $\sqrt{3}\times\sqrt{3}$-Ag structure in the RHEED pattern.[3,4]

The measurements were performed in an ultrahigh vacuum (UHV) chamber with a RHEED system, a sample holder for four-probe conductivity measurements, and an alumina-coated W basket as a Ag evaporator. The same experimental method as in previous reports[1,5,6] was adopted; the electrical resistance of the central portion of the wafer, under isothermal conditions at RT, was measured as a voltage drop between a pair of Ta wire contacts (5.6-mm separation), with a constant current of 10 μA supplied through the Ta end-clamp electrodes. The RHEED beam and a

 © 1997 The American Physical Society

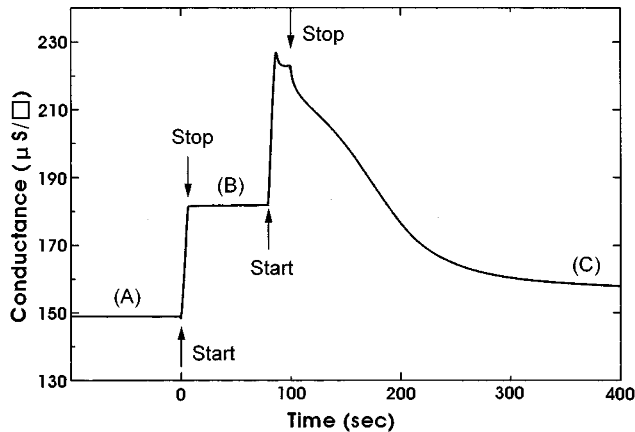

FIG. 1. Change in electrical conductance of a Si wafer with the Si(111)-$\sqrt{3}\times\sqrt{3}$-Ag surface at room temperature during the sequence of two successive Ag depositions onto it. The coverage of the first and second depositions were 0.022 ML and 0.066 ML, respectively. The deposition rate was 0.2 ML/min. (A)–(C) correspond to three samples used in the following photoemission measurements.

vacuum gauge were always turned off during the electrical measurements under a dark condition.

ARUPS and XPS were carried out in a separate UHV chamber equipped with a VG ADES 500 spectrometer. An angle-resolved analyzer was employed, which was of hemispherical type, rotating around two axes centered at the sample. An unpolarized He I (21.22 eV) light and a characteristic x ray of Mg K_α (1253.6 eV) were used for the photoelectron excitations. The energy resolution in our measurements was about 0.1 eV, estimated from the Fermi edge in a spectrum from the Ta clamp.

III. RESULTS

Figure 1 shows a conductance change of the Si wafer during the sequence of two successive Ag depositions onto the $\sqrt{3}\times\sqrt{3}$-Ag surface at RT. The conductance σ was calculated from the equation $\sigma=(1/R)(L/W)$, where R is the measured resistance between the pair of Ta wire contacts and L and W are the length and width of the measured area on the Si wafer, 5.6 mm and 3.7 mm, respectively. So the measured σ contains the contributions from both the bulk and surface. The same features as in previous reports[1,5,6] are seen. After the start of Ag deposition, the conductance steeply rises with the coverage. When the deposition is interrupted at 0.022 ML coverage, the conductance remains constant during the interruption period. It is interpreted that the deposited Ag atoms exist in a supersaturated metastable 2DAG phase, which makes the surface electrical conductance high.[1] When the second deposition (an additional 0.066 ML) is started, the conductance begins to rise again. Just after the Ag coverage exceeds a critical coverage for the nucleation Θ_C ($\sim$0.03 ML), a small overshoot is made.[1] When the deposition is interrupted again at 0.088 ML coverage in total, the conductance decreases steeply during the interruption period. This is because when the coverage is beyond Θ_C, the 2DAG begins to nucleate into 3D microcrystals, resulting in a reduction in the gas density down to a very small value equilibrated with the microcrystals.[1]

The conductances themselves for the clean 7×7 and the initial $\sqrt{3}\times\sqrt{3}$-Ag surfaces at RT were measured. The preparations and conductance measurements of these two structures were carried out alternately with a single Si wafer, while both conductances were simultaneously measured in single runs in a previous report.[7] After about 30-times flash heatings for cleaning the surface, the conductances for the 7 ×7 and $\sqrt{3}\times\sqrt{3}$-Ag surfaces were determined by averaging several measurements to be $\sigma_{7\times7}=111\pm7\,\mu$S/□ and $\sigma_{\sqrt{3}\times\sqrt{3}}=149\pm2\,\mu$S/□, respectively. So we can safely say that the difference $\Delta\sigma=\sigma_{\sqrt{3}\times\sqrt{3}}-\sigma_{7\times7}=38\pm8\,\mu$S/□ is only due to the difference in surface conductance.

To measure the evolution of surface electronic structures during the Ag depositions like in Fig. 1, ARUPS and XPS were carried out for three samples corresponding to (A) the initial $\sqrt{3}\times\sqrt{3}$-Ag surface, (B) after 0.022-ML-Ag deposition on sample (A), and (C) after further additional 0.066-ML-Ag deposition (0.088 ML in total) on sample (B). Sample (B) had a supersaturated metastable 2DAG of Ag on the surface, while sample (C) had negligible 2DAG due to its nucleation. The 2DAG on sample (B) could continue to exist while taking the photoemission spectra.[1] The XPS data from the Si $2p$ core level can be used to evaluate the surface E_F shifts because the energy of the emitted photoelectrons from the Si $2p$ level is higher than 1 keV, so that our measurements are bulk sensitive and free from surface chemical shifts. It is known that the surface E_F of the 7×7 surface lies 0.63 eV above the valence-band maximum (VBM), irrespective of the bulk impurity concentration.[8] Therefore, the binding energy of the Si $2p$ peak at the 7×7 surface could be used as a reference in determining the E_F positions at samples (A)–(C). The Si $2p$ peak from sample (A) shifts towards lower binding energy than that of the 7×7 clean surface by about 0.57 ± 0.05 eV, which is similar to the result

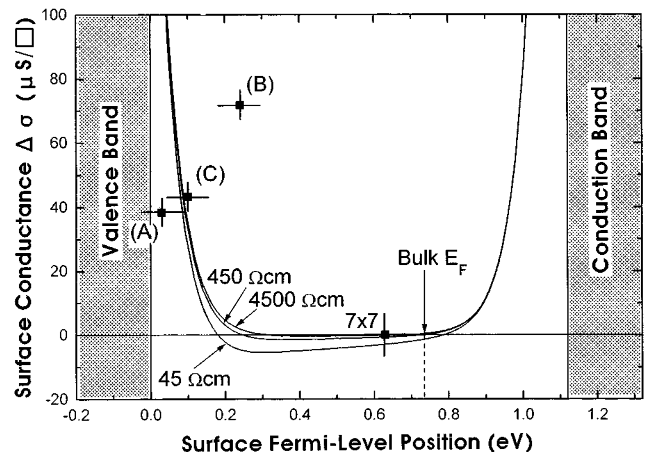

FIG. 2. Difference in surface conductance at samples (A)–(C) with respect to that of the 7×7 clean surface, measured by the four-probe method, plotted at the respective surface E_F positions determined by XPS measurements. Solid lines show the excess electrical conductances through the surface space-charge layer calculated as a function of the surface E_F position with different bulk resistivities. The conductance under the flat-band condition was defined as the reference. The 7×7 surface is assumed to have no extra conduction in addition to through the surface space-charge layer, so that the data point of the 7×7 surface is assumed to be on the calculated curves.

in Ref. 9, while the peak from sample (*B*) shifts back towards higher binding energy by 0.18 ± 0.05 eV than that of sample (*A*). Finally, sample (*C*) returns from sample (*B*) to nearly the same situation as for sample (*A*). The surface E_F positions determined in this way are plotted on the abscissa in Fig. 2. The ordinate in Fig. 2 shows the differences in surface conductance between the respective surfaces and the 7×7 surface. The conductances of samples (*B*) and (*C*) are obtained by comparing with that of sample (*A*) in Fig. 1. Sample (*A*) has a higher conductance than that of the 7×7 surface by $38\pm8\,\mu\mathrm{S}/\square$, as mentioned before.

In Fig. 3 ARUPS spectra from the three samples (*A*)–(*C*) are presented. The emission angles θ_e shown here correspond to a range of wave vectors around the $\bar{\Gamma}$ point ($\theta_e\approx36°$) in the second $\sqrt{3}\times\sqrt{3}$ surface Brillouin zone (SBZ). For sample (*A*), the same features as in a previous report[10] are reproduced. The dominant feature in the spectra is a surface state, designated S_1, close to E_F. With an energy gap below the S_1 state, the other peaks denoted S_2 and S_3 are observed. All the surface states $S_1\sim S_3$ gradually shift towards higher binding energy during the process of cooling the sample down to RT from a high temperature at which the $\sqrt{3}\times\sqrt{3}$-Ag structure had been prepared, as reported in Ref. 10. But the binding energies of these peaks become constant after 1 h. Figure 3(a) represents the results from the surface in such a steady state of the ''initial'' $\sqrt{3}\times\sqrt{3}$-Ag surface. These data are summarized in a two-dimensional band dispersion diagram in Fig. 4. The S_1 state disperses steeply around $\bar{\Gamma}$ point in the second SBZ. The bottom of the S_1 band at the $\bar{\Gamma}$ point is approximately 0.15 eV below E_F. For sample (*B*), as shown in Fig. 3(b), the same features as in Fig. 3(a) are observed in the spectra, but all the surface states shift by about 0.15 eV towards higher binding energy compared to the case of sample (*A*). The S_1-state peaks become more prominent well below E_F [Fig. 3(b)]. For sample (*C*), almost the same spectra are restored as sample (*A*); the spectra shift back by about 0.15 eV towards lower binding energy from sample (*B*) and the intensity of the S_1 state returns to be weaker.

IV. DISCUSSIONS

As the resistivity of the Si sample was measured to be stably $450\pm20\ \Omega$ cm, the E_F position in the bulk was estimated to be 0.73 eV above the VBM.[11] The band bending and the resulting excess carrier concentration in the surface space-charge layer can then be calculated by solving the Poisson equation.[12] The excess conductance through the surface space-charge layer is finally obtained as a function of the surface E_F position using the bulk parameters of the electron and hole mobilities. The results are shown as solid curves in Fig. 2 for different bulk resistivities. The contribution of the surface space-charge layer σ_{sc} to the surface conductance σ_s can be evaluated by these curves and accordingly we can estimate the surface-state conductance σ_{ss} by subtracting the calculated σ_{sc} from the measured σ_s.

It has been discussed that unintentional impurities, especially shallow acceptors by boron and deep-level impurities

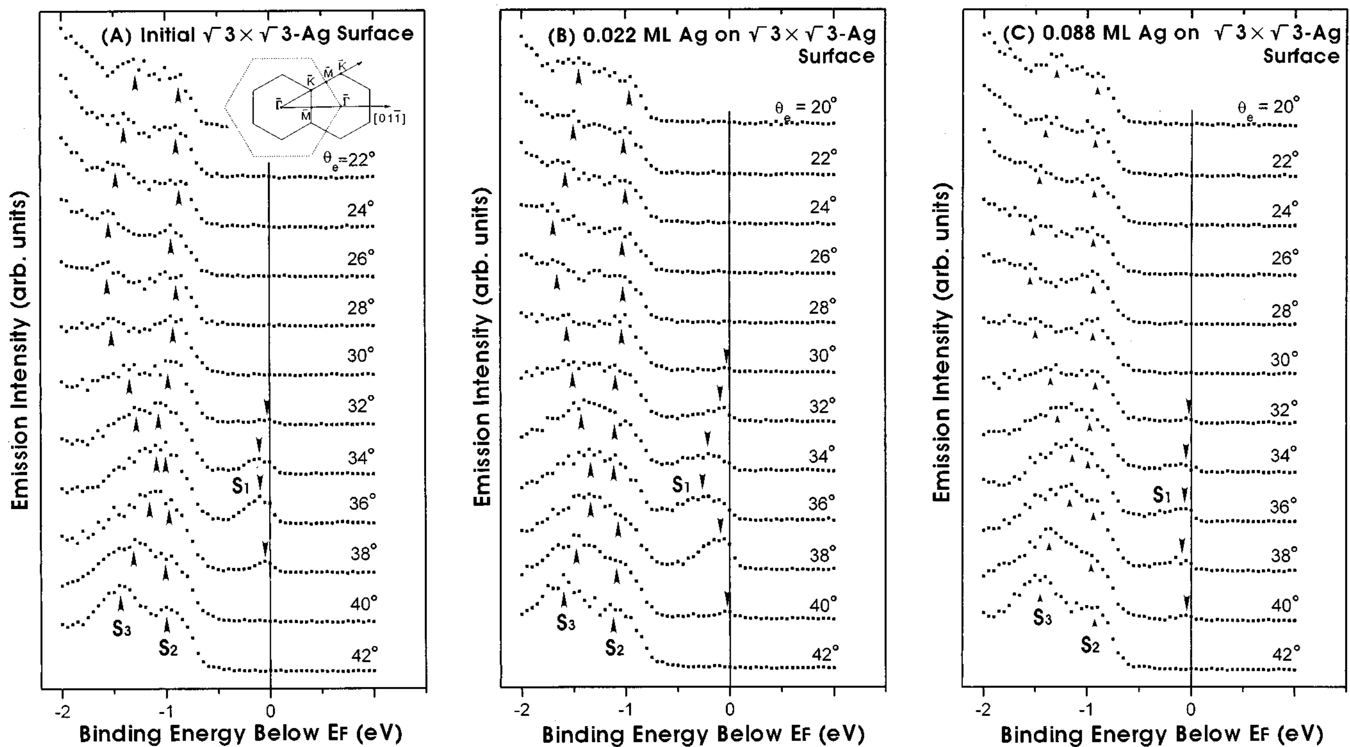

FIG. 3. ARUPS spectra for the samples corresponding to (*A*)–(*C*) in Fig. 1, scanned in [01$\bar{1}$] direction. The angle of incidence of the ultraviolet light of 21.2 eV was set 15° from the surface normal. The emission angles θ_e presented here, measured from the surface-normal direction, correspond to a range of wave vectors around the $\bar{\Gamma}$ point in the second $\sqrt{3}\times\sqrt{3}$ surface Brillouin zone (SBZ) (see the inset). We could not measure the spectra around the $\bar{\Gamma}$ point in the first SBZ because of a geometrical arrangement of the electron analyzer and UV source in our chamber. The emission intensity from the S_1 state has been measured to be very weak in the first SBZ (Ref. 10).

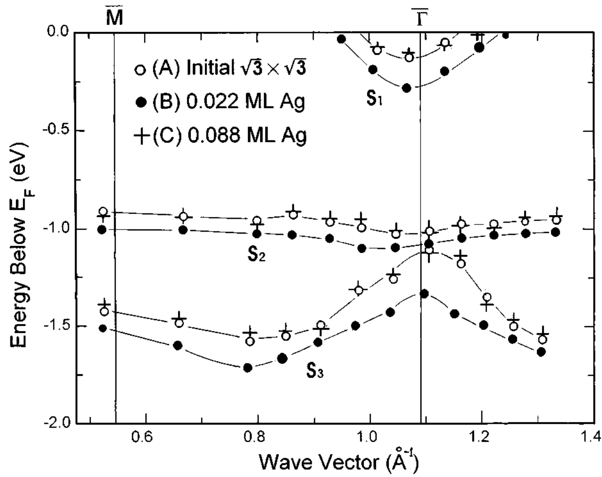

FIG. 4. Two-dimensional band dispersion diagram of the S_1, S_2, and S_3 surface states for the three samples (A)–(C) recorded in the $[01\bar{1}]$ direction, corresponding to the $\bar{\Gamma}$-$\bar{M}$-$\bar{\Gamma}$ direction in the $\sqrt{3}\times\sqrt{3}$ SBZ. This is constructed from the spectra in Fig. 3. Thin solid lines are to guide the eye.

of other elements, are easily introduced in Si wafers during high-temperature heating in UHV chambers.[13,14] This is the reason why the measured resistivity 450 ± 20 Ω cm is higher than the nominal value 11–100 Ω cm for our n-type Si wafers due to compensation. But the calculated excess surface conductance through the surface space-charge layer does not change so much even if the resistivity is higher (4500 Ω cm) or lower (45 Ω cm) than the measured value by an order of magnitude as seen in Fig. 2. Considering the uncertainty in the carrier mobilities in the surface space-charge layer, which may be lower than the bulk parameters due to carrier scattering at the surface, the errors in the conductance measurements, and the low resolution in our photoemission spectroscopies to determine the surface E_F positions, we can say that the data points for samples (A) and (C) are roughly on the calculated curves in Fig. 2. This means that measured conductances for samples (A) and (C) are explained mainly through the surface space-charge layer.

While sample (A) is under a hole-accumulated condition, the surface space-charge layer of sample (B) changes towards the flat-band condition, judged from the surface E_F shift, so that the excess holes are depleted. Therefore, the electrical conductance through the surface space-charge layer for sample (B) should be suppressed. On the contrary, the surface conductance was measured to increase from sample (A) to (B). Then this cannot be explained by conductance through the surface space-charge layer.

Sample (A) showed no significant surface-state conductance, resulting in its data point roughly on the calculated curves in Fig. 2, while the data point of sample (B) remarkably deviates from the curves, meaning the contribution of the surface-state conductance σ_{ss}. Considering that the S_1 surface state is highly dispersive, the energy shift of this surface state from at samples (A) to (B) (see Fig. 4) indicates that excess conductance at sample (B) comes from the excess electrons accumulated in the S_1-state band. The S_1 state of sample (B) is filled by more electrons than at sample (A) because of electron doping into the S_1 state by Ag adatoms in its 2DAG phase. The charge densities donated by 2DAG into the S_1 state and into the surface space-charge layer can be evaluated as follows.

The area in the $\sqrt{3}\times\sqrt{3}$ SBZ where the S_1 band fills can be estimated by assuming an isotropic dispersion of the band around $\bar{\Gamma}$. For sample (A), $(2.9\pm0.3)\%$ of the S_1 band is filled, which corresponds to a charge density in the surface state $Q_{ss}=-(1.6\pm0.3)\times10^{13}$ e/cm^2, where e is the elementary charge. On the other hand, the excess (positive) charge Q_{sc} in the surface space-charge layer of sample (A) is $(6\pm1)\times10^{11}$ e/cm^2, calculated from the measured surface-E_F position,[12] which is much smaller than $|Q_{ss}|$. Therefore, the extra donor-type surface states that are positively charged must exist to balance the neutrality. For sample (B), $(6.4\pm0.5)\%$ of the S_1 band is filled, meaning that the charge in the S_1 state is $Q_{ss}=-(3.5\pm0.6)\times10^{13}$ e/cm^2. Therefore, the charge doped into the S_1 band by the 2DAG is estimated to be $Q_{2\mathrm{DAG}\rightarrow S_1}=-(1.9\pm0.7)\times10^{13}$ e/cm^2. On the other hand, the charge transferred into the surface space-charge layer from the 2DAG is $Q_{2\mathrm{DAG}\rightarrow sc}=-(6\pm1)\times10^{11}$ e/cm^2, calculated from the measured surface-E_F position at sample (B). This means that the excess holes vanish almost completely by electron transfer from the 2DAG. The ratio of charges between in the S_1-state band and in the surface space-charge layer, donated from the 2DAG, is then $Q_{2\mathrm{DAG}\rightarrow S_1}:Q_{2\mathrm{DAG}\rightarrow sc}\approx30:1$. Consequently, the sum $Q_{2\mathrm{DAG}\rightarrow S_1}+Q_{2\mathrm{DAG}\rightarrow sc}=(1.9\pm0.7)\times10^{13}$ e/cm^2 corresponds to an electron density of 0.025 ML, using the definition of 1 ML$=7.83\times10^{14}$ cm^{-2}. This means that the charge transferred from the 2DAG (0.022 ML of Ag adatoms) into the substrate is estimated to be approximately one electron per a Ag adatom. This is equal to the number of Ag valence electrons (one) and then the Ag adatom must be positively monovalent ionized.

The dispersion of the S_1 band does not change significantly from sample (A) to (B), as shown in Fig. 4. The shift of the surface-state positions from sample (A) to (B) (approximately 0.15 eV) is the same as the change in band bending measured by XPS (about 0.18 eV). This means that the substrate structure does not change by 2DAG-Ag adsorption, so that any additional surface chemical shifts in ultraviolet photoemission spectroscopy are negligible.

The same measurements were done for a p-type Si(111) wafer of 20 Ω cm resistivity. Similar changes in the surface states and Si $2p$ core level were observed and the picture of electron doping into the S_1 band by Ag adatoms mentioned above was valid also for p-type samples.

Electromigration phenomena of Ag on the $\sqrt{3}\times\sqrt{3}$-Ag surface have been extensively studied.[15] The migration direction suggests that Ag adatoms on the surface are positively charged, which is consistent with our conclusion.

Since the dispersion of the S_1 band is nearly parabolic, we can expect it to be a 2D free-electron band, and the conductance due to the electrons in the S_1 band can be calculated by Boltzmann's approach. The conductance σ of a 2D free-electron system is given by $\sigma=S_F e^2 l/2\pi h$, where S_F is the circumference of the Fermi disk, l is the mean free path of electrons, and h is Planck's constant. For sample (B), using the Fermi wave number $k_F=0.15\pm0.02$ Å^{-1} obtained from

the band dispersion in Fig. 4 and the surface-state conductance 71±5 μS/□ estimated from Fig. 2, we obtain $l=14\pm2$ Å. Considering possible characteristic distances among carrier scattering centers (e.g., atomic steps and domain boundaries), the most frequent scatterings may be caused by Ag adatoms in the 2DAG. When the coverage of the 2DAG is 0.022 ML, the average distance among Ag adatoms is 27 Å if Ag adatoms are homogeneously distributed on the surface. Therefore, the estimated mean free path l is roughly equal to the average separation among the Ag adatoms, suggesting that the ionized Ag atoms in the 2DAG phase mainly act as carrier scattering centers.

The collision time τ for sample (B) is also calculated from the definition $l=\tau v$, where the Fermi velocity v_F is used for v. For the estimation of v_F, we used the Fermi wave number $k_F=0.15\pm0.02$ Å^{-1} and the effective mass $m^*=(2.6\pm0.4)\times10^{-31}$ kg ($=0.29\pm0.05m_e$, where m_e is the free electron's rest mass), which are derived from the dispersion of the S_1 band in Fig. 4. Then, $\tau=(2.3\pm0.3)\times10^{-15}$ s is obtained. Therefore, the mobility of electrons in the S_1 band is $\mu=e\tau/m^*=14\pm4$ cm^2/V s. This value is much smaller than the bulk parameter $\mu_{\text{bulk}}\sim1500$ cm^2/V s. This may be because of severe carrier scatterings by Ag adatoms in the 2DAG phase, defects, and domain boundaries of the $\sqrt{3}\times\sqrt{3}$-Ag superstructure.

Although the surface-state conduction through the S_1-state band should be expected also at the initial $\sqrt{3}\times\sqrt{3}$-Ag surface [sample (A)], it is not clearly confirmed, as shown in Fig. 2. If deep-level dopants, which may be caused during flashing the wafer in UHV, are introduced, the carrier density in the surface space-charge layer is reduced. This means that the calculated curves in Fig. 2 should be lowered so that the data point of sample (A) should be well above the curves. It will then turn out that there exists surface-state conduction also at sample (A).

For the initial $\sqrt{3}\times\sqrt{3}$-Ag surface prepared on p-type Si(111) wafers,[7] the measured surface conductance σ_S is larger than the calculated conductance σ_{SC} through the surface space-charge layer. It was suggested that this is due to conduction through the surface-state band. In Ref. 7 it was concluded that the difference in surface conductance $\Delta\sigma$ between the $\sqrt{3}\times\sqrt{3}$-Ag and the 7×7 clean surfaces is $\Delta\sigma=\sigma_{\sqrt{3}\times\sqrt{3}}-\sigma_{7\times7}=115\pm5\,\mu$S/□ for p-type wafers, which is larger than the value $\Delta\sigma=38\pm8\,\mu$S/□ obtained for an n-type wafer in the present study. On the other hand, the bottom of S_1-state band was measured in our ARUPS to be 0.13 eV for n type and 0.1 eV for p type below E_F, respectively. This means that the electron density filling the S_1-state band is slightly lower for p type than for n type. These results are opposite to the situation expected from the measured conductance $\Delta\sigma$ mentioned above. Then we have to say that it is difficult at the moment to quantitatively compare the surface-state conductions between the n-type and p-type samples, partially because the surface-state conductance may depend on the difference in surface-defects density due to different surface preparation procedures. Furthermore, the nature of filling the S_1 surface-state band, which should be empty according to the first-principles calculations,[16,17] is not yet completely clarified. Deep-level dopants, possibly introduced during thermal treatments, may play some roles in these problems.

Another issue to be discussed is the possible surface-state conductance at the 7×7 surface. In constructing Fig. 2 we have assumed that the data point for the 7×7 surface is on the calculated curves, meaning that only the electrical conduction through the surface space-charge layer is considered.[19] However, there are reports insisting an extra conductance of around 1 μS/□ due to the dangling-bond-state band on the 7×7 surface.[18] However, even if we include their conclusion in the analysis in Fig. 2, our conclusion is not significantly affected because of the much smaller surface-state conductance on the 7×7 surface compared to those of the $\sqrt{3}\times\sqrt{3}$-Ag surfaces.

ACKNOWLEDGMENTS

We acknowledge valuable discussions with Professor Martin Henzler of Hannover University and Professor Shozo Ino of Utsunomiya University. This work has been supported in part by Grants-In-Aid from the Ministry of Education, Science, Culture, and Sports of Japan, in particular through Creative Basic Research Program (No. 08NP1201) and International Scientific Research Program (No. 07044133) conducted by Professor Katsumichi Yagi of Tokyo Institute of Technology. We have been supported also by Core Research for Evolutional Science and Technology of the Japan Science and Technology Corporation conducted by Professor Masakazu Aono of Osaka University and RIKEN.

*Present address: ULSI Device Development Laboratories, NEC Corporation, Sagamihara, Kanagawa, Japan.

†Author to whom correspondence should be addressed. Electronic address: shuji@surface.phys.s.u-tokyo.ac.jp

‡Present address: Semiconductors Laboratory, The Institute of Physical and Chemical Research (RIKEN), Wako, Saitama, 351-01, Japan.

[1] Y. Nakajima, G. Uchida, T. Nagao, and S. Hasegawa, Phys. Rev. B **54**, 14 134 (1996).

[2] R. Schad, S. Heun, T. Heidenblut, and M. Henzler, Phys. Rev. B **45**, 11 430 (1992).

[3] S. Hasegawa, H. Daimon, and S. Ino, Surf. Sci. **186**, 138 (1987).

[4] T. Takahashi and S. Nakatani, Surf. Sci. **282**, 17 (1993), and references therein.

[5] S. Hasegawa and S. Ino, Phys. Rev. Lett. **68**, 1192 (1992); Surf. Sci. **283**, 438 (1993); Thin Solid Films **228**, 113 (1993).

[6] S. Hasegawa and S. Ino, Int. J. Mod. Phys. B **7**, 3817 (1993).

[7] C. S. Jiang, S. Hasegawa, and S. Ino, Phys. Rev. B **54**, 10 389 (1996).

[8] F. J. Himpsel, G. Hollinger, and R. A. Pollack, Phys. Rev. B **28**, 7014 (1983).

[9] S. Kono, K. Higashiyama, T. Kinoshita, T. Miyahara, H. Kato, H. Ohsawa, Y. Enta, F. Maeda, and Y. Yaegashi, Phys. Rev. Lett. **58**, 1555 (1987).

[10] L. S. O. Johansson, E. Landemark, C. J. Karlsson, and R. I. G. Uhrberg, Phys. Rev. Lett. **63**, 2092 (1989); **69**, 2451 (1992).

[11] S. M. Sze, *Physics of Semiconductor Devices* (Wiley, New York, 1981).

[12] C. E. Young, J. Appl. Phys. **32**, 329 (1961).

[13] L. He and H. Yasunaga, Jpn. J. Appl. Phys., Part 1 **24**, 928 (1985).
[14] M. Liehr, M. Renier, R. A. Wachnik, and G. S. Scilla, Jpn. J. Appl. Phys., Part 1 **61**, 4619 (1987).
[15] H. Yasunaga, Surf. Sci. **242**, 171 (1991); H. Yasunaga and A. Natori, Surf. Sci. Rep. **15**, 205 (1992).
[16] Y. G. Ding, C. T. Chan, and K. M. Ho, Phys. Rev. Lett. **67**, 1454 (1991); **69**, 2452 (1992).
[17] S. Watanabe, M. Aono, and M. Tsukada, Phys. Rev. B **44**, 8330 (1991).
[18] Y. Hasegawa, I.-W. Lyo, and Ph. Avouris, Appl. Surf. Sci. **76/77**, 347 (1994); in *Ultimate Limits of Fabrication and Measurement*, edited by M. E. Welland and J. K. Gimzewski (Kluwer, Dordrecht, 1995), pp. 147–153.
[19] V. A. Gasparov and K. R. Nikolaev, Phys. Low-Dim. Struct. **1/2**, 53 (1996).